Characterization Methodology for Biological Plywoods Based on Characteristic Cross-Section Patterns

Oscar F. Aguilar Gutierrez and Alejandro D. Rey*

Department of Chemical Engineering, McGill University, 3610 University Street, Montreal, Quebec, H3A 0C5, Canada

Received February 12, 2016; Accepted May 31, 2016

ABSTRACT: Biological plywoods are solid analogues of liquid crystalline phases whose building blocks, including cellulose, collagen and chitin, present multifunctionality, providing in some cases protection, camouflage, self-healing and/or adaptability to the surrounding environment. The 3D ordered structure is the main factor for these fascinating properties, and the assessment of the structure-property relationship will be a powerful tool in terms of future material design and innovation. Cross-section observations lead to characteristic patterns depending on the specific arrangement of the plywood's building blocks. Twisted plywood architectures, known as the Bouligand structure, lead to the widely observed arced patterns which can be ideal or nonideal depending on whether the relationship between the twist angle and the spatial coordinate is linear or not. The latter is the case of nonideal and the projected arcs to the incision plane do not have a constant periodicity. On the other hand, orthogonal plywoods project into herringbone patterns when the incision angle is adequate. In either case, arcs or herringbones, key characteristic variables, have been identified that provide quantitative means that relate them to structural variables such as the pitch and the helix location. Based on this quantitative information we proposed a methodology to characterize the plywoods when these characteristic patterns are accessible. The method has been validated using *in-vivo* and *in-silico* observations, where the latter were obtained using Mayavi, a general purpose 3D visualization software. In this article we present a new analysis of plywoods' mechanics using Krenchel's formalism and we give a broad and unifying vision of our recent findings regarding cross-section reconstruction techniques of several biological plywoods along with recommendations that increase accuracy in the predictions.

KEYWORDS: Biological liquid crystals, cross-section patterns, biological plywoods

1 INTRODUCTION

Structural macromolecules, such as collagen, chitin and cellulose, are nature's building blocks to create a wide variety of architectures showing multiscale organization. Such architectures are usually obtained through an efficient entropy-driven self-assembly [1–3] that can be an equilibrium or non-equilibrium process. These building blocks have fibrillar shape and rigidity in common, crucial requirements for liquid crystalline self-assembly processes. Additionally, geometric and chemical chirality is present at the molecular level, manifesting in the macroscopic chirality [4] which is widely observed in biological systems. Self-assembly of biological polymers, such as collagen, was observed *in vitro* without the intervention of any tissue-specific cells [5], which established an analogy between biological materials and conventional liquid crystals. Biological materials where liquid crystalline self-assembly processes are present are known as biological liquid crystals (BLCs) and can be classified into three main categories: i) solid analogues or biological plywoods (BPs), ii) *in-vitro* solutions, and iii) *in-vivo* materials and secretions. Table 1 shows examples of the three categories of BLCs along with the references for more information regarding types ii and iii since they are out of the scope of this paper. Biological plywoods are solid materials that exhibit the organization of a liquid crystal, however the building blocks cannot move freely due to a loss of mobility, a consequence of an evaporation and/or crosslinking process [6, 7]. But the organized structure follows a previous liquid crystalline self-assembly process. Examples of these materials include insect cuticles, bone osteons, nails, among others [3, 8–10]. From the morphogenesis point of view, there are two main paths that lead to a BP: a) equilibrium and b) non-equilibrium processes.

*Corresponding author: alejandro.rey@mcgill.ca

DOI: 10.7569/JRM.2016.634119

© 2016 Scrivener Publishing LLC

Table 1 Biological plywoods and respective building blocks.

Nematic Plywood	TPA (Ideal and Nonideal)	Orthogonal Plywood
Intermediate layer in beetle cuticle (chitin) [15]	Crab cutible [10]	*Eremosphera viridis* cell wall (cellulose) [17]
Nails (keratin) [8]	Endocarp of plums, *prunus sativum* (cellulose) [16]	*Paralvinella grasslei* (annelid) cuticle (collagen) [18]
Tendon fibrils (collagen) [5]	Aerenchyma cell wall (cellulose) [16]	*Pagrus major* scales (collagen) [19]
	Stone cells in pears, *pyrus malus* (cellulose) [16]	*Oryctes rhinoceros* eggshell (chitin) [20]
	Bone osteons (collagen)	Bird cornea (several species) (collagen) [21]

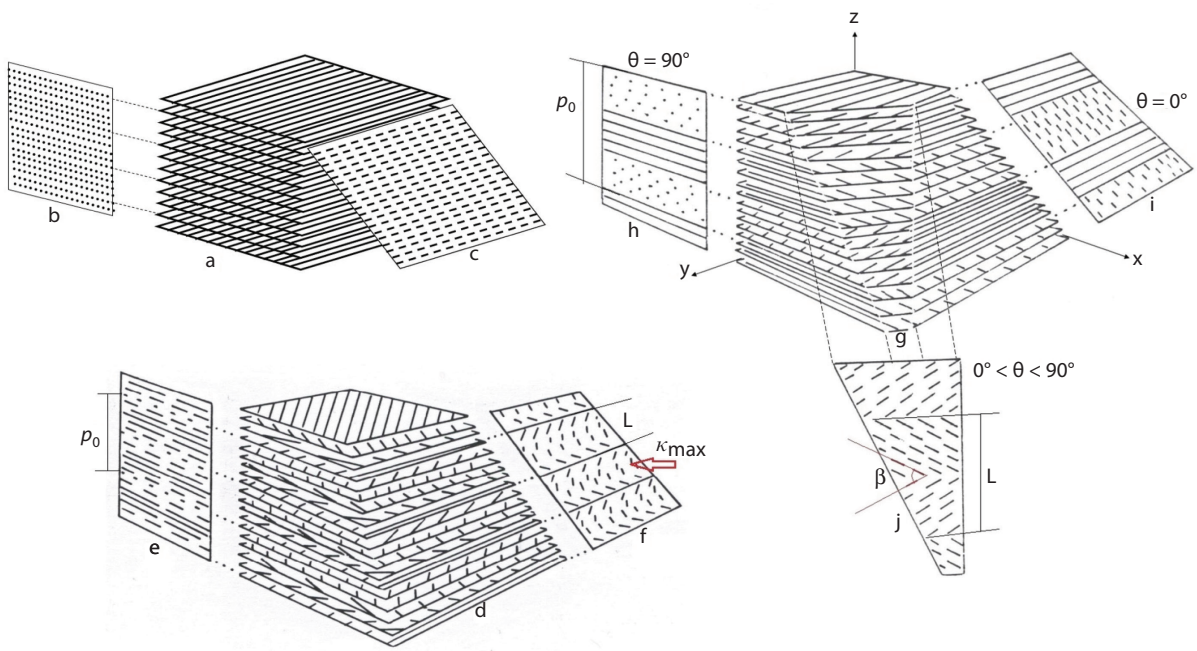

Figure 1 Representation of the nematic plywood (**a**–**c**) with one preferred orientation of the fibrils throughout the full plywood showing oblique incisions leading to dots (**b**) when the incision is orthogonal to the fibril alignment and a series of parallel lines (**c**) with any other angle; helical plywood (TPA) (**d**–**f**) where the cholesteric arrangement with characteristic pitch p_0 is shown (**d**) and projections corresponding to the periodic pattern with periodicity of $p_0/2$ (**e**) and the arced pattern in oblique incisions with characteristic periodicity L and maximum curvature k_{max} (**f**) and the orthogonal plywood (**g**–**j**) showing layers orthogonally arranged with projections where no characteristic pattern is identified (**h**–**i**) and the herringbone pattern with characteristic periodicity L and aperture or herringbone angle β with a rotation of the oblique incisions (**j**). (Adapted from [23])

During the former, the self-assembly is directed by a chiral front propagation towards the isotropic phase; with the appropriate anchoring conditions this leads to a defect-free material [6]. While the latter requires the synchronization of several transport processes that might include coating flows and evaporation of water in order to induce a phase transition towards a liquid crystalline behavior while at the same time losing the mobility of the respective building block [11]. It is worth mentioning that of the two types of morphogenesis, equilibrium self-assembly has received more attention from the experimental and theoretical [6, 12, 13] point of view, while the non-equilibrium process still remains to be explored or is in development [14]. Advantages for choosing the non-equilibrium over the equilibrium process are the relatively shorter times required for the formation of the plywood and its possibility for scaling to engineering production once the principles are established.

Common types of organizations in these plywoods are the nematic, helical and orthogonal, shown in Figure 1. By taking an incision of any of the presented

© 2016 Scrivener Publishing LLC

plywoods, the full 3D fibrillar organization is projected into the incision plane and in carefully selected cases it leads to a qualitative knowledge of the full 3D structure. For example, arced patterns observed by cross-sectional projections are a fingerprint of the helical plywood. Other types of plywoods will lead to different types of projections in orthogonal plywoods such as dots, segments or other distinctive patterns such as herringbones. A quantitative pattern analysis procedure gave rise to the structural characterization of these composites, where unknown variables such as the pitch and the helix orientation can be obtained from characteristic variables of the projected patterns: periodicity and curvature for the arcs and periodicity and herringbone angle for herringbone patterns. It is important to note that in any case the characterization depends on a single variable since the projection is a function of the slicing angle, and an additional variable is required to remove this degree of freedom.

The organization of this article is as follows. Section 1.1 presents a brief discussion regarding biological plywoods, their 3D organization, the structure-property relationships with the analysis of mechanical responses of biological plywoods using Krenchel's formalism, and the cross-section characterization scheme is given. The geometric models are then presented in Section 2 for the two most important biological plywoods, followed by the general material characterization methodology. Section 3 presents *in-vivo* and *in-silico* applications previously reported [11, 22, 23] and validation results. Then recommendations on the applicability of the methodology to increase the precision in the predictions are presented and discussed.

In this article we present a broad and unifying vision of our recent findings [22, 23] regarding cross-section reconstruction techniques of several biological plywoods along with recommendations that increase accuracy in the predictions.

1.1 Plywood Architectures

In this section we describe the specific organization of three types of plywoods: i) Nematic, ii) Cholesteric, and iii) Orthogonal, and identify the relationship of each fibrillar organization with the specific set of multifunctionalities. The specific variables that appear in oblique sections of the cholesteric and orthogonal cases are the dependence on the incision angle and the description of the inverse problem where the output (the patterns) is used to describe the input (the full 3D structure).

Nematic plywoods have fibril arrangements that resemble nematic liquid crystals, where only orientational order exists. This type of plywood can be found throughout the entire material sample and also as an intermediate layer, as in the case of some beetles where a uniaxial layer separates two cholesteric layers. This nematic layer plays the role of a "half-wave plate," changing the helicity of incident light [15]. The projections obtained by oblique incisions lead to a family of parallel lines showing only one preferred orientation when the incision plane lies between the values of 0° and 90°, as observed in Figure 1. The length of the projected lines are between the length of the fibrils at 0° and decreases as the angle approaches the upper limit until dots are obtained and no characteristic pattern is associated with this type plywood.

Helical plywoods (known as twisted plywood architecture or TPAs) present a fibril arrangement similar to a cholesteric liquid crystal, which is regarded as a collection of nematic planes but presenting a twist in the orientation between adjacent planes. Associated with this type of material is the cholesteric pitch p_0, which is a characteristic length scale associated with the distance required by the fibrils to undergo a full rotation. These were the first types of plywoods to be identified when Bouligand [10] observed arced patterns in oblique sections of crab cuticle which indicated the presence of a helical arrangement of chitin. Helical plywoods can present ideal or nonideal arrangements that depend on if the relationship between the twist angle θ and the space coordinate is linear or not, i.e., space varying pitch. This has been observed in the endocarps of some fruits where a double pitch system was identified [16] which can be identified as a linear relationship in a piece-wise fashion; another example of nonideal plywood is the cuticle of some beetle species showing increases and decreases in the pitch [9]. Oblique incisions to these materials project into arcs that may have a constant periodicity throughout the entire sample plane for ideal plywoods or with varying periodicity for the nonideal. The periodicity of the projected arcs depends on the incision angle; such an effect was observed in goniometric studies [16], which leads to different periodicity in the arcs for a constant pitch by moving the incision angle. In order to avoid this apparent ambiguity, an auxiliary variable is required to directly correlate the pitch with the incision angle which is the curvature of the arcs for TPAs, which will be detailed in the following section.

Orthogonal plywoods present several groups of layers with the same orientation within individual layers, but with an abrupt change in the orientation of 90° between each one [23]. It can be seen as a particular case of the nonideal TPAs, where a staircase function defines the space-dependent pitch, however it is convenient to define it separately; but a pitch can still be defined for these materials, as in TPAs. Other angles have been reported for these materials ranging

 © 2016 Scrivener Publishing LLC

between 45° and 90° and are denominated as quasi-orthogonal plywoods. Additionally, the paired orthogonal has also been observed which consists of a pair of adjacent layers that are oriented orthogonally and the subsequent set of pairs show a smooth rotation which leads to nested arced patterns [24]. These arrangements have been found in certain algae cell walls, in collagen-based materials reinforced with mineral compounds in fish scales [19, 21] and in bone osteons in planar and cylindrical configurations [1, 21, 25, 26]. Another remarkable example is the cornea of certain species, where collagen fibrils are assembled in an orthogonal fashion in the stroma, composing approximately 90% of the cornea thickness. For the classic orthogonal plywoods, oblique incisions with a suitable combination of the polar (ϕ) and azimuthal (θ) angles, as depicted in Figure 1(g-j), lead to the herringbone patterns. When one of the fibrils' orientation lies in any of the coordinate axes associated with the incision plane (θ = 0 or 90°) no patterns are observed but parallel layers with dots and parallel lines are observed, whose lengths depend on the orientation of the plane. Avoiding this scenario (i.e., 0° < θ < 90°) leads to the herringbone patterns, and for the particular case of 45°, symmetric herringbone angles are obtained since the two orthogonal sets of fibrils are shifted equally from the axis associated with the incision plane resulting in the same projected length. Even when the azimuthal angle is fixed, changes in the polar angle will project a different angle in the herringbones for the same material, and a strong similarity is observed with TPAs, and the variable that allows closure in this situation is the herringbone angle.

Each of these two plywoods has its own set of multifunctionalities because each arrangement provides different mechanical/optical response. Some optical properties have been computed theoretically for ideal and nonideal helical plywoods; for further information the reader is referred to [27, 28]. In terms of mechanical properties, when an anisotropic material is submitted to stresses, the response of the material depends on the orientation of the fibrils. This was recognized by Krenchel in laminated materials and defined an efficiency factor η depending on the orientation of the applied stress with respect to the fiber orientation. Such expression can be adapted to biological plywoods [21] and is given in Equation 1:

$$\eta = \sum_{i}^{N} M_i \cos^4 \phi_i \quad (1)$$

where M_i is the number fraction of fibers at an angle with respect to the direction of tension and ϕ its relative orientation with respect to the applied stress. To better understand this relationship and how it affects the stiffness we give the following Table 2, where the efficiency factor is computed for some limiting cases and the consequences of such values are identified. Additionally, Figure 2 shows a schematic of the data presented in Table 2.

In terms of the efficiency, TPAs are better suited for supporting loads and stresses and these materials are commonly found in peripheral body locations [21, 29]. In arthropods, epicuticles have been found to present helical arrangements, and besides providing protection these materials are also involved in other processes such as water regulation [21], thermal regulation [15] and even pheromone recognition. Plant cell walls are also required to resist pressures and stresses and also exhibit helicoidal configurations [13].

Table 2 Krenchel efficiency factor evaluation for biological plywoods (see Figure 2).

Plywood type and orientation with respect to applied stress	Efficiency factor (Eq.1)	Mechanical property impact
Nematic Plywood. Stress is applied parallel to the fiber orientation	1	The efficiency factor has its maximum value
Nematic Plywood. Stress is applied perpendicular to the fiber orientation	0	The efficiency factor has its minimum value
Orthogonal Plywood. Stress is applied parallel to one of the groups of fibers orientation	0.5	The efficiency factor does not present its maximum value because half of the group of fibers is not aligned with the stress
Orthogonal Plywood. Stress is applied at 45° from any of the two orthogonal orientations	0.25	The efficiency factor presents a lower value than the previous case, however in any case drops to zero, as in the nematic plywood
Helical Plywood. Stress is applied at any angle	0.375	The efficiency factor does not present a value close to the maximum but is indifferent with respect to the direction of the application of the stress

© 2016 Scrivener Publishing LLC

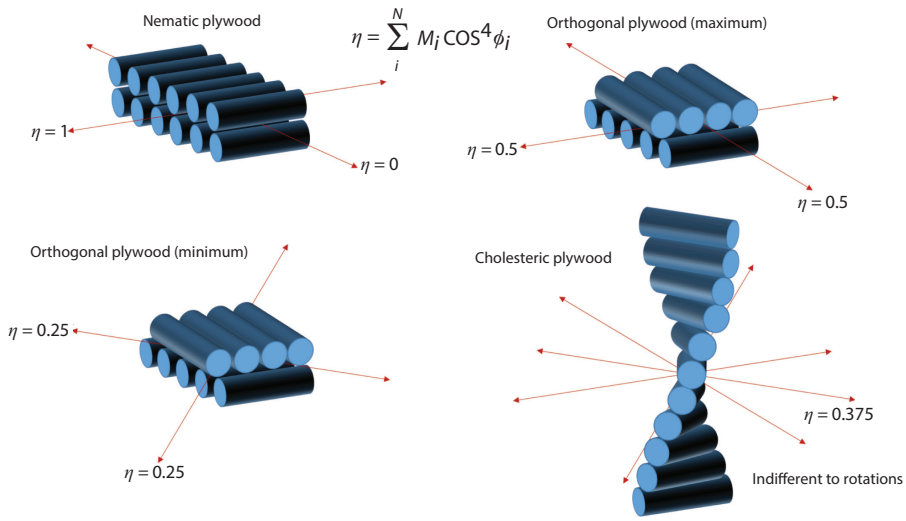

Figure 2 Summary of the cases analyzed with Krenchel's formula explained in Table 2; the directions of the applied stress are indicated with the red lines.

On the other hand, orthogonal arrangements can provide the necessary strength [30], and one of the main functionalities is to preserve the shape via a "lazy-tongs" mechanism [21]. The fibril arrangement is responsible for balancing loads, as observed in laminated composites [31], and also for the mechanical failure mechanism consisting of the sliding of the lamellae before the fibers fracture individually as observed in fish scales [19]. The orthogonal plywood also plays an important role in the self-healing process, where reversible transitions from orthogonal to randomly oriented occur in connective tissue [21]. Orthogonal plywoods present important optical properties, where the stroma is responsible for nearly 2/3 of the optical power of the eye [30].

The presented evidence strongly suggests a crucial structure-property relationship; however it has not been fully understood. Prior to achieving a full understanding, an assessment of the morphology of plywoods is required and robust characterization techniques are also desired. Cross sections presenting characteristic patterns provide an interesting alternative for these purposes. What is crucial in these cross sections is to unambiguously correlate measurable quantities from the 2D observations to unknowns, such as the pitch, avoiding multiple solutions that may arise given that the incision angle is, in principle, unknown. The geometric model that will be detailed in the following section is capable of providing this information and a methodology based upon it is given as well. Using additional computational tools, the full 3D structure can be reconstructed and used for more extensive computer simulation work or *in-silico* experiments.

2 GEOMETRIC MODEL

2.1 Ideal and Nonideal TPA

The director field of a cholesteric liquid crystal $\underline{n} = (\cos(2\pi z/p_o), \sin(2\pi z/p_o), 0)$ is projected to an incision plane located at an angle whose orientation is given by the angle "α" as shown in Figure 3. The projected vector field is now $\underline{u} = \underline{u}(\alpha,s)$ and the streamlines in such plane define the trajectories of the projections in such plane and are given by Equation 2:

$$\frac{dx}{ds} = \frac{\cot\left[\dfrac{2\pi(\sin\alpha)s}{p_0}\right]}{\cos\alpha} \tag{2}$$

The solution of such an equation is a periodic function whose 2D periodicity (L) depends on α and p_0, where a linear relationship between the L and p_0 is extracted:

$$L = \frac{p_0}{2\sin\alpha} \tag{3}$$

In order to use Equation 3 to calculate the pitch p_0 from a measured periodicity L, the angle α must be known, which is generally unknown, and hence an auxiliary variable is needed that does not introduce an additional unknown. The curvature of the arcs was used and it was determined that the maximum curvature, which occurs in the center of the arcs, depends on α and L only:

$$\kappa_{\max} = \frac{\pi}{L\cos\alpha} \tag{4}$$

© 2016 Scrivener Publishing LLC

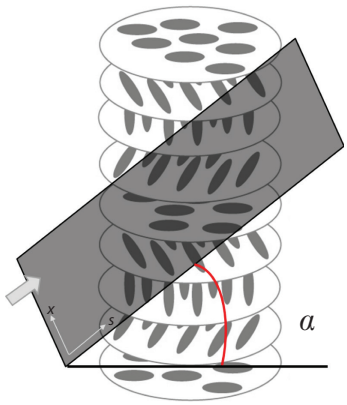

Figure 3 Schematic representation of the helix axis oriented in the z direction and the incision plane with orientation given by α.

Equations 3 and 4 provide a complete description of the arced patterns for a given incision angle leading to Equation 5. In the case of nonideal structures, different values of L found in a sample will provide the particular value of p_0 at a given place in the space when the angle is calculated with one of the arcs found in the plane. Equations 3 and 4 can be combined into a single Equation 5 that describes the phase diagram of L - k_{max} for a constant pitch. This combined Equation 5 leads to a family of hyperbolas whose asymptotes represent small angle incisions which imply ill-conditioning (i.e., small fluctuations as inputs lead to large changes in the output), showing that these incisions should be avoided for accuracy (see [22] for details).

$$\left(\frac{2}{p_0}\right)^2 L^2 - \left(\frac{2\pi}{p_0}\right)^2 \frac{1}{\kappa_{\max}^2} = 1 \tag{5}$$

2.2 Orthogonal Plywoods and Characterization Methodology

Given the similarity of the problem with the arc patterns of twisted plywoods, by using the geometry shown in Figure 4 an equivalent expression for the orthogonal plywoods is obtained:

$$L = \frac{p_0}{2\sin\alpha} \tag{6}$$

The auxiliary variable for closure in the case of these plywoods is the herringbone angle β (see herringbone pattern on the bottom right panel of Figure 1). This angle is obtained by taking the dot product of the projection of two orthonormal vectors to a plane with orientation given by a unit normal vector $\underline{k}$, as observed in Figure 4 (right).

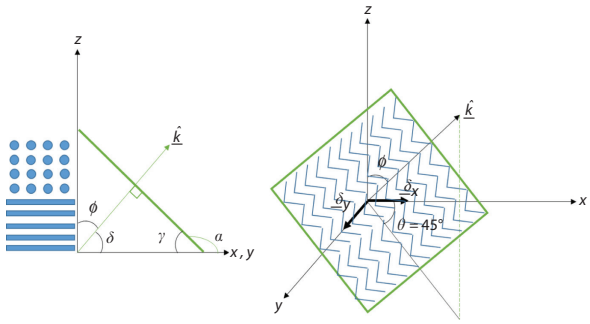

Figure 4 Schematic representation of the orthogonal plywood fibril orientation (first panel from the left) and the projection to an incision plane locate at an angle "α" (right), and details on the incision plane with orientation given by unit normal vector $\underline{k}$ (right panels). The herringbone angle β is shown at the bottom of Figure 1.

$$\underline{\delta}_x^{\,p} \cdot \underline{\delta}_y^{\,p} = |\underline{\delta}_x^{\,p}|\,|\underline{\delta}_y^{\,p}|\cos\beta = (\hat{\underline{\delta}}_x - k_x\hat{\underline{k}}) \cdot (\hat{\underline{\delta}}_y - k_y\hat{\underline{k}}) \tag{7}$$

By assuming symmetric herringbone patterns ($\theta = 45°$) the final expression that relates β and α is:

$$\cos\beta = \frac{-\sin^2\alpha}{1+\cos^2\alpha} \tag{8}$$

Equations 6 and 8 are analogous expressions for orthogonal plywoods that provide a full description of the observed patterns and both sets of expressions can be used to characterize materials where a characteristic two-dimensional pattern is observed in cross sections. The methodology proposed in this work for the determination of three-dimensional fibrillary structure in helical and orthogonal plywoods is as follows:

1. Examine the cross section and determine if arced (herringbone) patterns are visible;
2. Measure L and k_{max} (β) from the arced (herringbone) patterns;
3. Calculate α from Equation 4 (Eq. 8);
4. Estimate pitch p_0 from Equation 3.

At the end of the 1-to-4 sequence, a full knowledge of the fibrillar composite structure is obtained.

3 EXAMPLES

3.1 Arced Patterns Description and Chiral Graded Structure (*C. Aurigans* Scarab)

Figure 5 shows solutions to Equation 2 for different values of p_0 and different values of α. In experimental goniometric studies, different observation angles

© 2016 Scrivener Publishing LLC

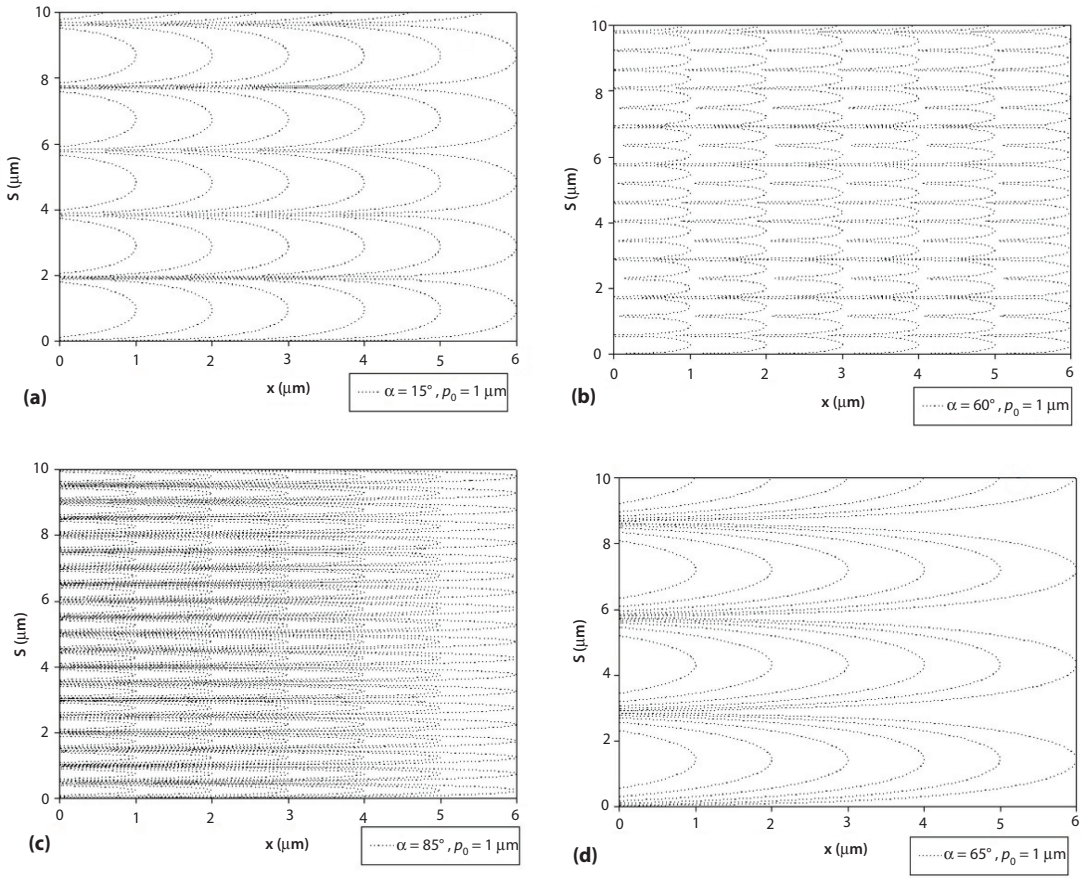

Figure 5 Parametric solutions to Equation 2 showing the evolution of the arcs by changing the incision angle (**a**–**c**) and the effect of changing the pitch (**b**–**d**).

are used to detect how the arc patterns are modified. In our simulation case the observation angle remains constant but different values of α in Equation 2 simulate the same effect. The geometric model describes the evolution of the arcs and the characterization procedure can be applied. The methodology has been validated *in silico* by creating synthetic arced patterns due to the lack of experimental cross sections. A pitch profile reported in the literature [9] was used in Mayavi to create this visualization and the incision angle can be manipulated. Three different values of the incision angle were chosen (15, 25 and 40°), two of which are shown in Figure 6, and the methodology was applied to obtain the pitch predictions. The comparison between the three predictions and the experimental value are given in Figure 7. It is worth remarking that higher angles lead to better predictions and a larger region is reconstructed since more information of the helical axis is included in the incision plane.

3.2 Orthogonal Plywoods (Algae Cell Wall)

Due to the lack of experimental information regarding the orthogonal plywoods, *in-silico* herringbone patterns are shown instead, showing the effect of moving the incision angle when the pitch remains constant in Figure 8. This demonstrates that the geometric model describes the evolution of these characteristic patterns and the methodology for characterizing is applicable in these situations. The methodology has been applied to *in-silico* patterns to validate the methodology (details can be found in [23]), where it was shown that the larger source of error is the measurement of the periodicity of the structures. A biological validation was carried out as well with *in-vivo* samples where herringbone patterns are observed in cross sections of the cell wall of the algae species *Eremosphera viridis*. The cell wall thickness was calculated from the number of layers

 © 2016 Scrivener Publishing LLC

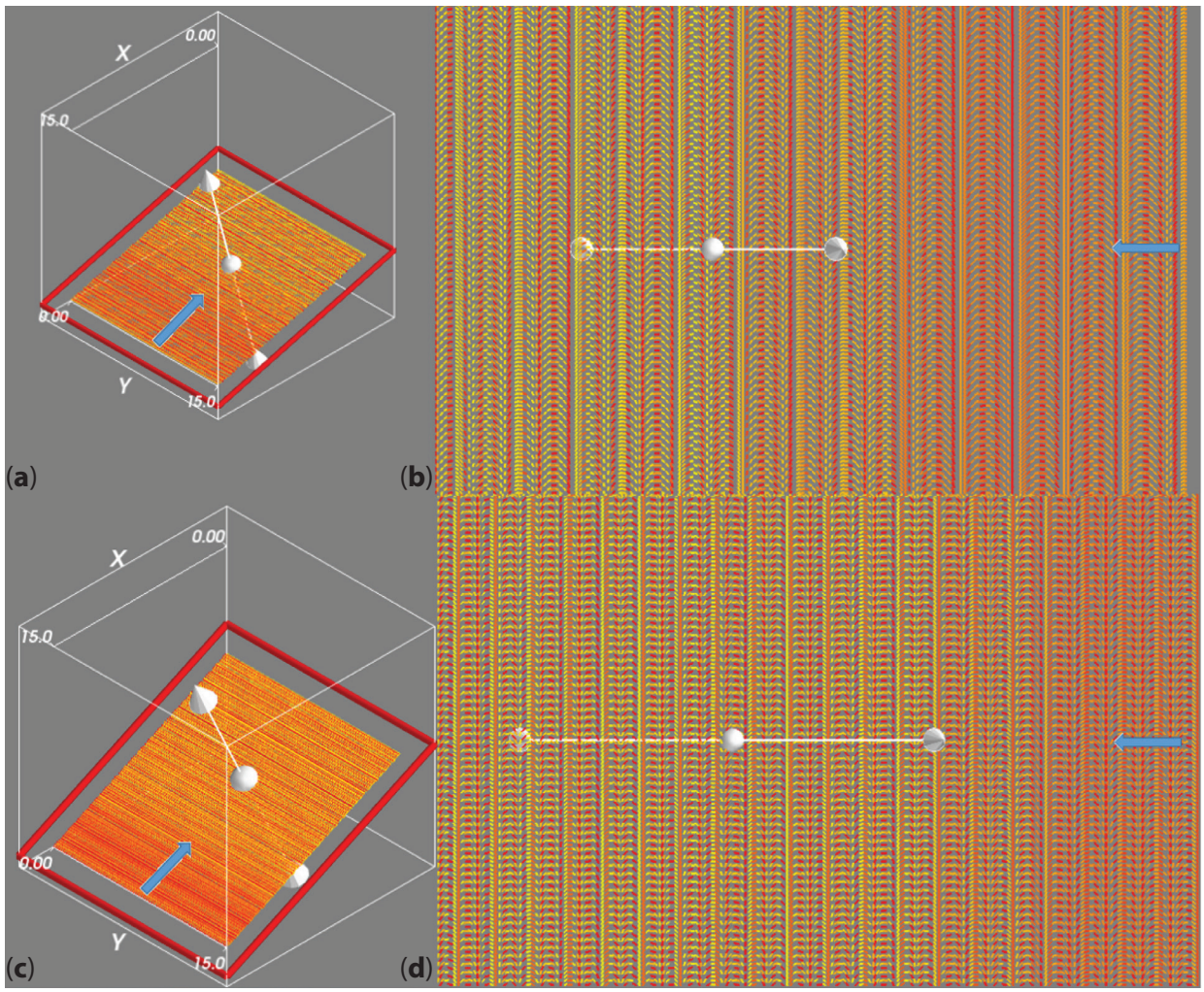

Figure 6 *In-silico* arced patterns for the *C. aurigans* scarab cuticle showing two different incision angles: 15° (**a**–**b**) and 25° (**c**–**d**). The arrows are placed as reference only.

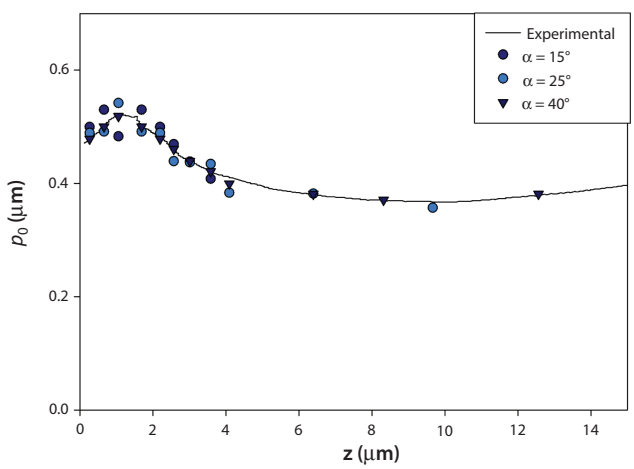

Figure 7 Pitch profile predictions compared to the experimental values [9] for the three chosen incision angles.

© 2016 Scrivener Publishing LLC

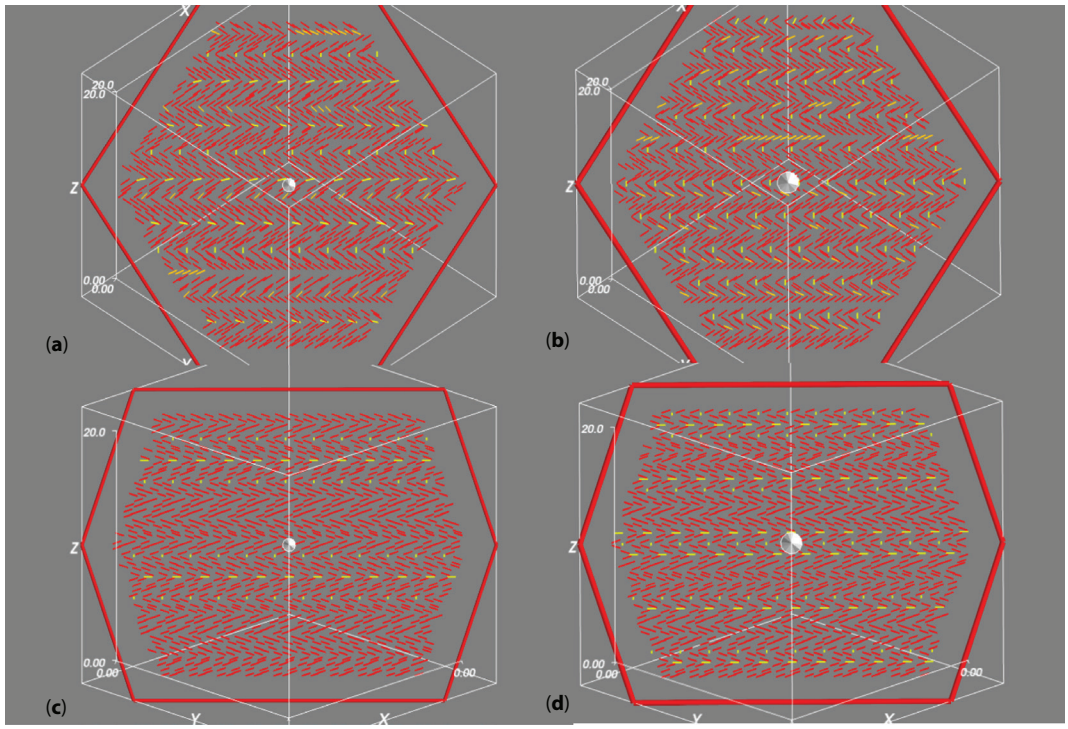

Figure 8 *In-silico* herringbone patterns for constant pitch p_o = 4 μm (**a**–**b**) and 6 μm (**c**–**d**) showing the change in L with po and α, but constant β for different p_o and the same α.

that compose the cell wall multiplied by $p_0/4$. The value obtained by applying the proposed methodology is 0.5236 μm compared to the experimental value of 0.5303 μm, showing a good agreement between the two values.

The source of errors in the methodology is the precision in the measurements of the patterns' variables and also the value of the incision angle, as mentioned in the previous section. An error analysis in [23] demonstrated that small incision angles should be avoided in both cases and for the case of orthogonal plywoods, the most sensitive parameter is the periodicity, meaning that small fluctuations in the measured value introduce a larger error and the predictions become less accurate.

4 CONCLUSIONS

Krenchel's formalism was adapted for the first time to shed light on the mechanics of biological plywoods (Table 2 and Figure 2), including the mechanical advantages of helical plywoods to other types, such as orthogonal or nematic, to support arbitrary loads.

The general overview given in this article identifies cross-sectional patterns as good candidates to obtain the full 3D structure in helical and orthogonal plywoods. A methodology based on analytic results from a geometric model was presented and is applicable when characteristic patterns such as herringbones or arced patterns are visible in an oblique incision of a biological plywood. The methodology has been validated for ideal and nonideal helical plywoods and also for orthogonal plywoods via *in-silico* created plywoods and with experimental observations.

The results show a good agreement between the calculated pitch profile for the nonideal plywood case (Figure 7) and with the calculation of the cell wall thickness for the case of the orthogonal plywood (see Section 3.2). The results presented here are part of a research program [32] in the structure-property relationship in biological plywoods and provide a new tool for further theoretical and experimental research in biological liquid crystal analogues such as cornea, bone and muscle tissues.

ACKNOWLEDGMENTS

This research was supported by a grant from the Natural Sciences and Engineering Council of Canada. OFAG is grateful for the financial support from CONACyT (Government of Mexico, scholarship number 313480).

 © 2016 Scrivener Publishing LLC

REFERENCES

1. P. Fratzl, Cellulose and collagen: From fibres to tissues. *Curr. Opin. Colloid Interface Sci.* **8**(1), 32–39 (2003).
2. D. Eglin, G. Mosser, M.M. Giraud-Guille, J. Livage, and T. Coradin, Type I collagen, a versatile liquid crystal biological template for silica structuration from nano- to microscopic scales. *Soft Matter* **1**, 129–131 (2005).
3. M.M. Giraud Guille, G. Mosser, C. Helary, and D. Eglin, Bone matrix like assemblies of collagen: From liquid crystals to gels and biomimetic materials. *Micron.* **36**(7), 602–608 (2005).
4. A.D. Rey, Liquid crystal models of biological materials and processes. *Soft Matter* **6**, 3402–3429 (2010).
5. E. Belamie, G. Mosser, F. Gobeaux, M.M. Giraud-Guille, Possible transient liquid crystal phase during the laying out of connective tissues: Alpha-chitin and collagen as models. *J. Phys. Condens. Matter* **18**(13), S115 (2006).
6. G. de Luca and A.D. Rey, Chiral front propagation in liquid-crystalline materials: Formation of the planar monodomain twisted plywood architecture of biological fibrous composites. *Phys. Rev. E Stat. Nonlin. Soft Matter Phys.* **69**, 011706 (2004).
7. G. de Luca and A.D. Rey, Monodomain and polydomain helicoids in chiral liquid-crystalline phases and their biological analogues. *Eur. J. Phys. E. Soft Matter* **12**, 291–302 (2003).
8. B. Forslind and M. Lindberg, *Skin, Hair and Nails*, pp. 21–54, 377–390, Taylor and Francis (2005).
9. E. Libby, D.E. Azofeifa, M. Hernández-Jiménez, C. Barboza-Aguilar, A. Solís, I. García-Aguilar, L. Arce-Marenco, A. Hernández, and W.E. Vargas, Light reflection by the cuticle of *C. aurigans* scarabs: A biological broadband reflector of left handed circularly polarized light. *J. Optics.* **16**, 082001 (2014).
10. Y. Bouligand, Twisted fibrous arrangements in biological materials and cholesteric mesophases. *Tissue Cell* **4**(2), 189–217 (1972).
11. O.F. Aguilar Gutierrez and A.D. Rey, Structure characterisation method for ideal and non-ideal twisted plywoods. *Soft Matter* **10**, 9446–9453 (2014).
12. Y. Murugesan, D. Pasini, and A.D. Rey, Defect textures in polygonal arrangements of cylindrical inclusions in cholesteric liquid crystal matrices. *Soft Matter* **9**, 1054–1065 (2013).
13. Y. Murugesan and A.D. Rey, Modeling textural processes during self-assembly of plant-based chiral-nematic liquid crystals. *Polymers* **2**(4), 766–785 (2010).
14. A.D. Rey and E.E. Herrera-Valencia, Liquid crystal models of biological materials and silk spinning. *Biopolymers* **97**(6), 374–396 (2012).
15. K. Allavherdyan, T. Galstian, A. Gevorgyan, and R. Hakobyan, Could the cuticle of beetles serve also for their radiative thermoregulation? *Optics Photonics J.* **3**(7A), 17–22 (2013).
16. J.C. Roland, D. Reis, B. Vian, B. Satiat-Jeunemaitre, and M. Mosiniak, Morphogenesis of plant cell walls at the supramolecular level: Internal geometry and versatility of helicoidal expression. *Protoplasma* **140**(2), 75–91 (1987).
17. M. Weidinger and H.G. Ruppel, Ca^{2+} requirement for a blue-light-induced chloroplast translocation in *Eremosphaera viridis*. *Protoplasma* **124**(3), 184–187 (1985).
18. L. Lepecheux, Spatial organization of collagen in annelid cuticle: Order and defects. *Biol. Cell* **62**, 17–31, (1988).
19. T. Ikoma, H. Kobayashi, J. Tanaka, D. Walsh, and S. Mann, Microstructure, mechanical and biomimetic properties of fish scales from *Pagrus major*. *J. Struct. Biol.* **142**, 327–333 (2003).
20. P.J.S. Furneaux and A.L. Mackay, *The Insect Integument*, H.R. Hepburn (Ed.), pp. 157–176, Elsevier (1976).
21. A.C. Neville, *Biology of Fibrous Composites*, pp. 85–120, Cambridge University Press, Cambridge, MA (1993).
22. O.F. Aguilar Gutierrez and A.D. Rey, Chiral graded structures in biological plywoods and in the beetle cuticle. *Coll. Inter. Sci. Comm.* **3**, 18–22 (2014).
23. O.F. Aguilar Gutierrez and A.D. Rey, Geometric reconstruction of biological orthogonal plywoods. *Soft Matter* **12**, 1184–1191 (2016).
24. M.M. Giraud-Guille, J. Castanet, F.J. Meunier, and Y. ouligand, The fibrous structure of coelacanth scales: A twisted plywood. *Tissue Cell* **10**, 671–686 (1978).
25. P. Fratzl and M.M. Giraud-Guille, *Hierarchy in Natural Materials*, Wiley-VCH Verlag GmbH & Co. KGaA (2011).
26. M.M. Giraud Guille, Twisted plywood architecture of collagen fibrils in human compact bone osteons. *Calc. Tissue Intern.* **42**(3), 167–180 (1988).
27. P. Rofouie, D. Pasini, and A.D. Rey, Tunable nanowrinkling of chiral surfaces: Structure and diffraction optics. *J. Chem. Phys.* **143**, 114701 (2015).
28. P. Rofouie, D. Pasini, and A.D. Rey, Nanostructured free surfaces in plant-based plywoods drivel by hiral capillartiry. *Coll. Inter. Sci. Comm.* **1**, 23–26 (2014).
29. A.C. Neville, *Biology of the Arthropode Cuticle*, Springer-Verlag (1975).
30. S.L. Wilson, A.J. El Haj, and Y. Yang, Control of scar tissue formation in the cornea: Strategies in clinical and corneal tissue engineering. *J. Funct. Biomater.* **3**(3), 642–687 (2012).
31. F.C. Campbell, *Structural Composite Materials*, ASM International (2010).[32] Y. Murugesan, D. Pasini, and A.D. Rey, Self-assembly mechanisms in plant cell wall components. *J. Renew. Mater.* **3**(1) 56–72 (2015).

© 2016 Scrivener Publishing LLC